Chemistry of Metals and Alloys

Chem. Met. Alloys 1 (2008) 24-33
Ivan Franko National University of Lviv
www.chemetal-journal.org

Structures and crystal chemistry of MT_6X_6 phases, filled derivatives of the CoSn-B35 structure

G. VENTURINI[1]*, H. IHOU-MOUKO[1], C. LEFÈVRE[2], S. LIDIN[3], B. MALAMAN[1], T. MAZET[1], J. TOBOLA[4], A. VERNIÈRE[1]

[1] *Laboratoire de Chimie du Solide Minéral, Université Henri Poincaré-Nancy I, associé au CNRS (UMR 7555), B.P. 239, 54506 Vandoeuvre les Nancy Cedex, France*
[2] *Max-Planck Institut für Festkörperforschung, D 70569 Stuttgart, Germany*
[3] *Arrhenius Laboratory, Department of Physical, Inorganic and Structural Chemistry, Stockholm University, 10691 Stockholm, Sweden*
[4] *Faculty of Physics and Nuclear Techniques, AGH University of Science and Technology, Al. Mickiewicza 30, 30-059 Kraków, Poland*
* *Corresponding author. E-mail: gerard.venturini@lcsm.uhp-nancy.fr*

Received December 21, 2007; accepted January 9, 2008; available on-line March 31, 2008

M atoms can be inserted into the host CoSn-type TX structure to give MT_6X_6 structures (M = Li, Mg, Ca, IIIA, IVA, lanthanides, U; T = Cr-Ni, X = Si, Ge, X' = Ga, In). The crystal structures of known MT_6X_6 compounds are reviewed and sorted into orthorhombic, monoclinic and hexagonal series. The diffraction results for ternary and pseudo-ternary compounds are summarized and discussed on the basis of preponderant M-X, T-X and M-T bonding. The structural evolutions in the pseudo-ternary compounds $MT_6X_{6-x}X'_x$ as a function of X' are analyzed, underlining the role of the size and electronic structure of X'.

Crystal chemistry / Crystal structure / Host structure / Intermetallics

1. Introduction

The MT_6X_6 compounds and $MT_6X_{6-x}X'_x$ pseudo-ternary compounds (M = Li, Mg, Ca, IIIA, IVA, lanthanides, U; T = Cr-Ni, X = Si, Ge, X' = Ga, In) have been studied by many research groups for their interesting and various physical properties [1-22]. Most of the studied compounds are isotypic to hexagonal $HfFe_6Ge_6$, but others crystallize in different orthorhombic superstructures. From a crystallographic point of view, all of them derive from the binary CoSn host structure through different filling schemes.

2. Crystal structures

2.1. The CoSn host structure and the filling process

The hexagonal CoSn structure [23] is a stacking of hexagonal Sn_2 planes and Co Kagomé planes with the hexagons centered by Sn_1 atoms. The Sn_2 atoms are located in cobalt trigonal prisms sharing edges in the (001) planes and faces along the [001] direction, building hexagonal channels occupied by the Sn_1 atoms (Fig. 1). The cobalt atoms are situated in tin octahedrons sharing faces in the (001) plane and edges along the [001] direction. This arrangement yields the formation of large empty hexagonal bi-pyramids. Taking into account a small deviation of the atoms at the apex of the bi-pyramids, this hole is suitable to guest large metallic atoms M, giving rise to the formula MT_6X_6. The relative height of the atoms M in the hexagonal channels leads to the different superstructures that will be described below. Typical diffraction patterns are shown in Fig. 2, which displays the diffracted intensities of some pseudo-ternary $LuFe_6Ge_{6-x}Ga_x$ compounds.

2.2. The $HfFe_6Ge_6$ and $ScFe_6Ga_6$-type structures

There exist two relatively simple structures corresponding to the formula MT_6X_6: the hexagonal $HfFe_6Ge_6$ type [24] (also called $MgFe_6Ge_6$ or $(Fe,Mn)_7Ge_6$ [25,26]) and the orthorhombic $ScFe_6Ga_6$ type [27], which should be regarded as a ternary derivative of the tetragonal $ThMn_{12}$ type [28]. In the $HfFe_6Ge_6$ type, the M atoms are all located in the same (001) planes and there is an alternate stacking of filled and empty planes (Fig. 3), while in the $ScFe_6Ga_6$ type, the planes (110) are alternately filled and empty. These arrangements lead to different capping of the trigonal prisms: mono- or bi-capped for the $ScFe_6Ga_6$ type and uncapped or tri-capped for the $HfFe_6Ge_6$ type. It will be shown later that all the superstructures

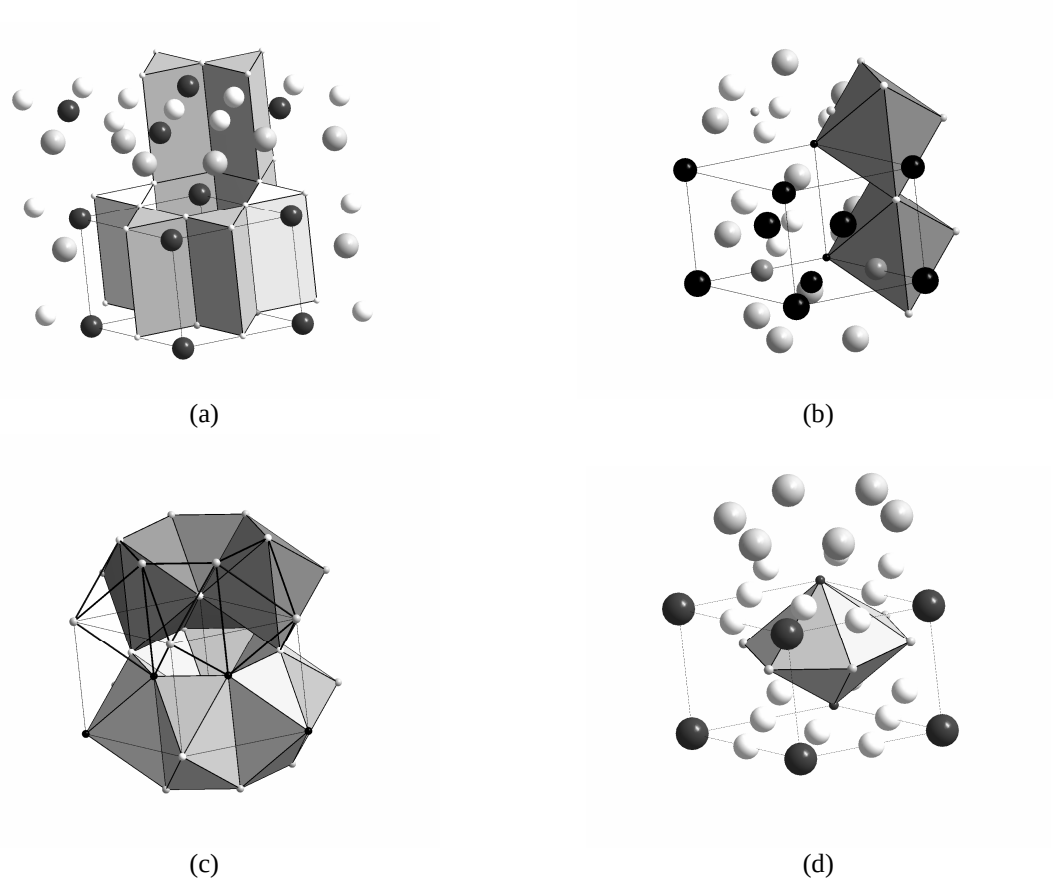

Fig. 1 The CoSn structure: trigonal prisms around the Sn_2 atoms (a); octahedrons around the Co atoms (b); hexagonal rings of octahedrons (c); empty hexagonal bi-pyramid (d).

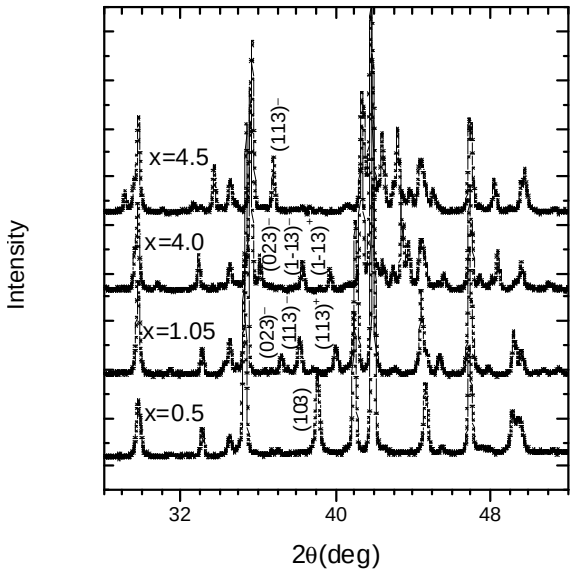

Fig. 2 Typical X-ray patterns of the $LuFe_6Ge_{6-x}Ga_x$ series: hexagonal $HfFe_6Ge_6$ type (x = 0.5); orthorhombic superstructure (x = 1.05); monoclinic superstructure (x = 4.0); orthorhombic $ScFe_6Ga_6$ type (x = 4.5).

can be regarded as different combinations of $HfFe_6Ge_6$- and $ScFe_6Ga_6$-units.

2.3. The orthorhombic series

The indexation of the diffraction patterns of the compounds belonging to the orthorhombic series is done considering the superstructure lines as satellites of the typical lines of the $HfFe_6Ge_6$ structure (*hkl*, *l* odd) and a propagating vector Q = (0, q_y, 0) (with respect to the ortho-hexagonal $HfFe_6Ge_6$ cell $a_o = a_h$; $b_o = a_h\sqrt{3}$; $c_o = 2c_h$) [29,30]. It has always been possible to relate the component q_y to a ratio of integers: q_y = n/p giving rise to the supercell parameters $a_s = a_h$; $b_s = p*a_h\sqrt{3}$; $c_s = 2c_h$.

The *z* coordinates of the M atoms, namely their relative height in the hexagonal channels, are related to the sign of the expression C = $\cos(2\pi*q_y*y_M)$, where y_M is the position of M in the successive ortho-hexagonal cells along the propagating direction. The coordinate z_M is equal to 0 and ½, respectively, for C positive and negative (in case of C = 0, the sign of sine is considered in the same way). The space group deduced from the atomic positions may also be derived from the parity of n and p, i.e. *Cmcm* for n odd and p even, *Cmmm* for n even and p odd, *Immm* for n and p odd.

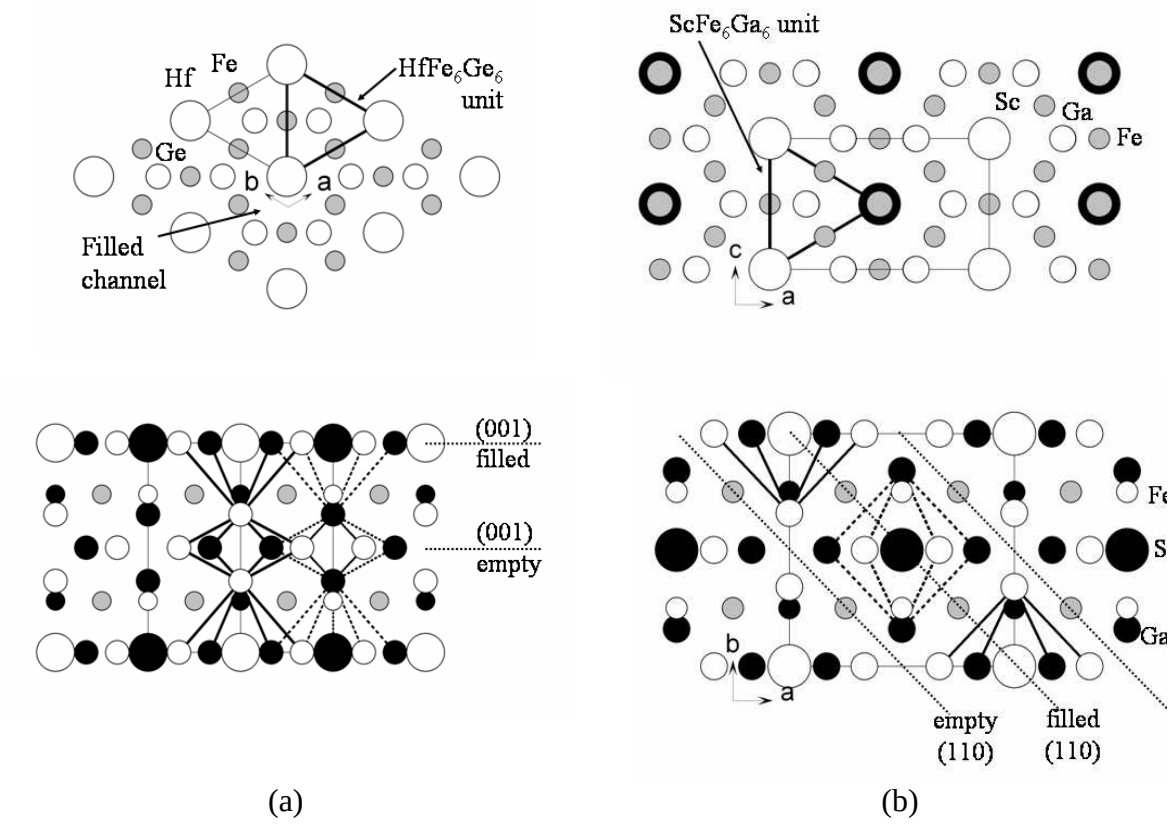

Fig. 3 Projections of the $HfFe_6Ge_6$- (a) and $ScFe_6Ga_6$-type (b) structures.

Projections of the known structures are given in Fig. 4. They may be described as infinite $HfFe_6Ge_6$ (H) and $ScFe_6Ga_6$ (S) slabs of different thickness, stacked along the propagating direction. The sequence of the slabs is also formulated in Table 1. It may be calculated that the concentration in $ScFe_6Ga_6$ slabs (S) is given by the value of the propagating vector component q_y [$S/(S+H) = q_y = n/p$].

2.4. The monoclinic series

In this series, the indexation of the diffraction patterns is done considering a two-component propagating vector $Q = (q_x, q_y, 0)$. In this case, the *z* coordinates of the M atoms are related to the sign of the expression $C = \cos(2\pi(q_x*x_M+q_y*y_M))$, where x_M and y_M are the coordinates of the M atoms in the (001) plane [31,32]. Two space groups deduced from the atomic positions have been recognized so far: *C*2/*m* and *P*2/*m*, where the pseudo-hexagonal axis becomes the unique axis. The concentration of $ScFe_6Ga_6$-units is also related to the components of the propagating vector through the relation $S/(S+H) = q_x+q_y$. Six sets of propagating vector components have been clearly established (Table 2). Four of them reasonably account for a commensurate model and the corresponding structures are gathered in Fig. 5. They display $HfFe_6Ge_6$-columns constituted of 2, 4 and 6 units, elongated along the unique axis and separated

Table 1 Summary of crystallographic data of the orthorhombic series.

	q_y	n/p	Space group	Sequence
$ErFe_6Sn_6$	0.25	1/4	*Cmcm*	H^3S^1
$ScFe_6Ge_{2.5}Ga_{3.5}$	0.268	3/11	*Immm*	$2(H^3S^1)H^2S^1$
$HoFe_6Sn_6$	0.333	1/3	*Immm*	H^2S^1
YFe_6Sn_6	0.375	3/8	*Cmcm*	$2(H^2S^1)H^1S^1$
$DyFe_6Sn_6$	0.400	2/5	*Cmmm*	$H^2S^1H^1S^1$
$TbFe_6Sn_6$	0.500	1/2	*Cmcm*	H^1S^1
$TbFe_6Ge_{3.5}Ga_{2.5}$	0.667	2/3	*Cmmm*	H^1S^2
$TbFe_6Ge_3Ga_3$	0.706	12/17	*Cmmm*	$2(H^1S^2)H^1S^3H^1S^2H^1S^3$

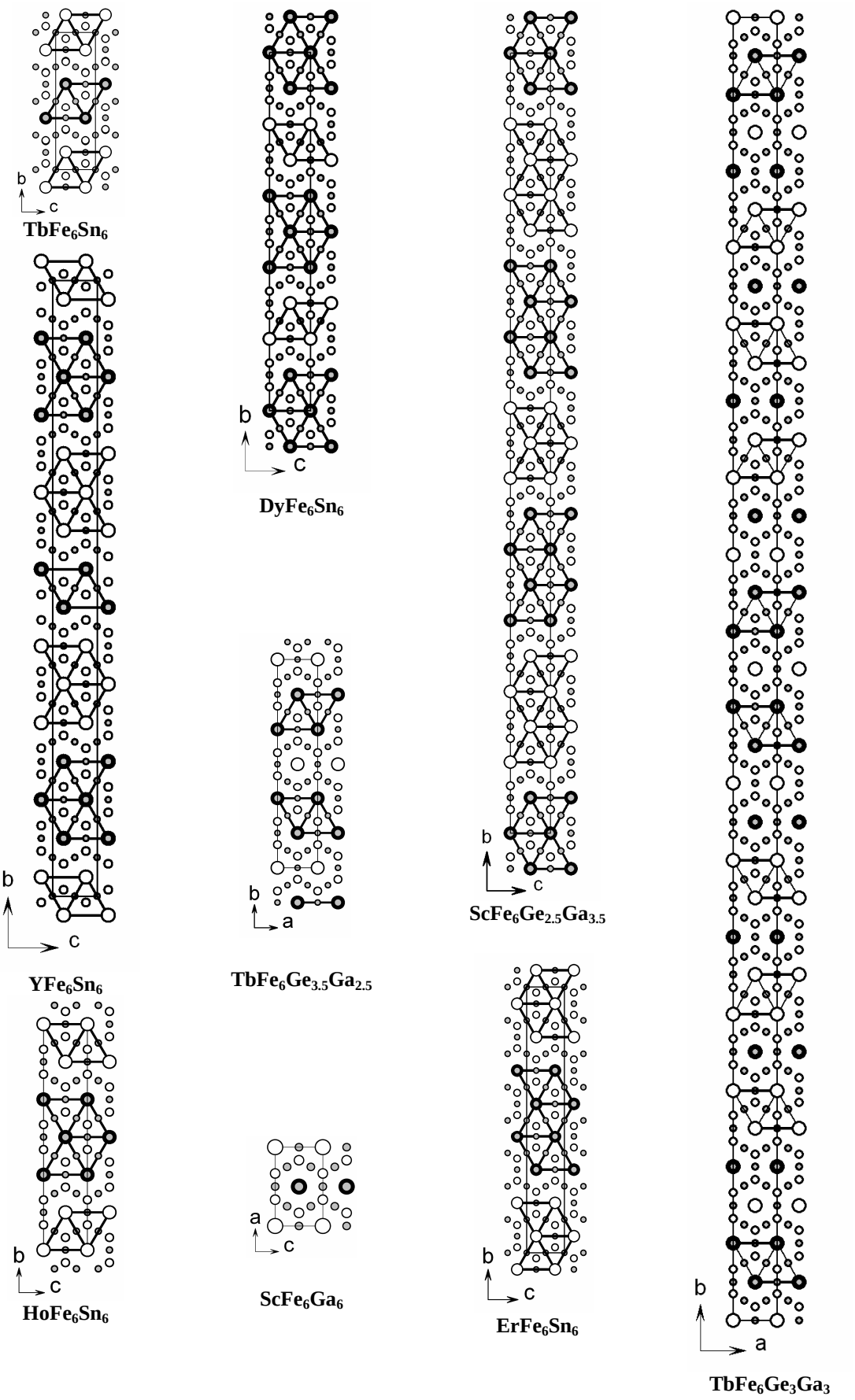

Fig. 4 Projections along the pseudo-hexagonal axis of the structures belonging to the orthorhombic series.

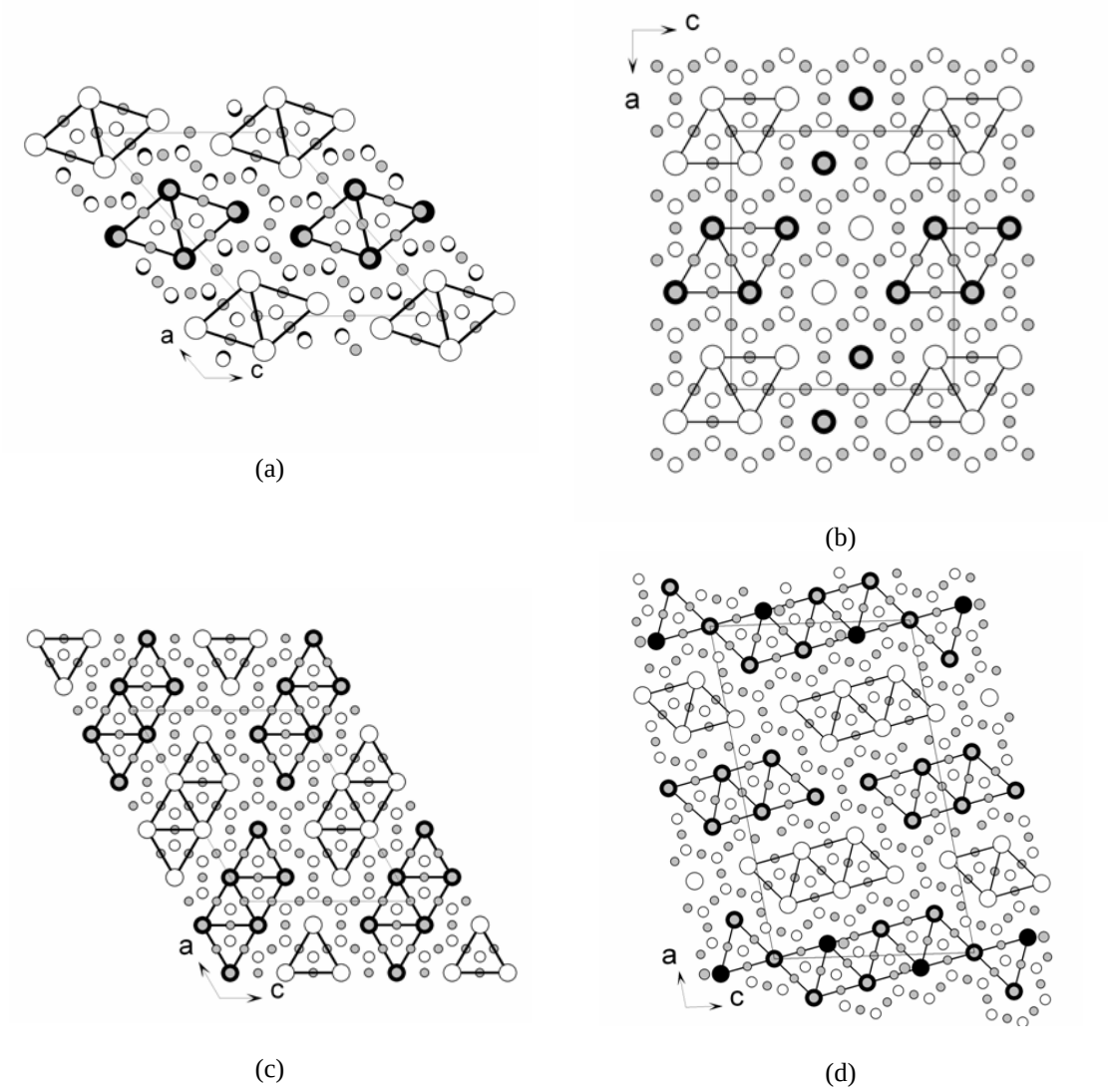

Fig. 5 Projections along [001] of the structures belonging to the monoclinic series: $LuFe_6Ge_2Ga_4$ (a), $ScFe_6GeGa_5$ (b), $TbFe_6Ge_4Ga_2$ (c),$TbFe_6Ge_{4.25}Ga_{1.75}$ (d).

Table 2 Summary of the crystallographic data of the monoclinic series.

	q_x	q_y	n_x/p_x	n_y/p_y	Σq_i
$ScFe_6Ge_{1.5}Ga_{4.5}$	0.232	0.403	3/13	2/5	0.635
$TbFe_6Ge_{4.25}Ga_{1.75}$	0.241	0.400	6/25	2/5	0.641
$LuFe_6Ge_{2.5}Ga_{3.5}$	0.244	0.420	11/45	21/50	0.664
$TbFe_6Ge_4Ge_2$	0.247	0.422	1/4	5/12	0.669
$LuFe_6Ge_2Ga_4$	0.249	0.500	1/4	1/2	0.749
$ScFe_6GeGa_5$	0.334	0.496	1/3	1/2	0.830

by $ScFe_6Ga_6$-units. Two of them, $LuFe_6Ge_2Ga_4$ and $ScFe_6GeGa_5$, display the same type of column, more or less diluted into the $ScFe_6Ga_6$ matrix.

Attempts have been made to analyze one of the compounds in the superspace model using the JANA program [33]. The refined components are q_x = 0.2440(3) and q_y = 0.4198(4). The structure, presented in Fig. 6, is mainly constituted of isolated columns of four $HfFe_6Ge_6$-units and therefore close to the $TbFe_6Ge_4Ga_2$ structure.

2.5. The hexagonal series

Hexagonal superstructures of the CoSn type have been known for a long time (Fig. 7). The $LiFe_6Ge_6$-type (*P*6/*mmm*; $a = \sqrt{3}\,a_h$; $c = 2c_h$) [34], like the $ScFe_6Ga_6$ type, does not display $HfFe_6Ge_6$ units

(S/[H+S] = 1). The $ScNi_6Ge_6$-type (*P*6/*mmm*; $a = 2a_h$; $c = 2c_h$) [35] displays hexagonal rings of $HfFe_6Ge_6$ units (S/[H+S] = 0.75). Both types, together with the $HfFe_6Ge_6$ type, may be considered as the first terms of a hypothetical hexagonal series, whose next terms might be characterized by an increasing parameter: $a = \sqrt{7}\ a_h$, $a = 3a_h$ and of course by an increasing number of combinations of the structural units.

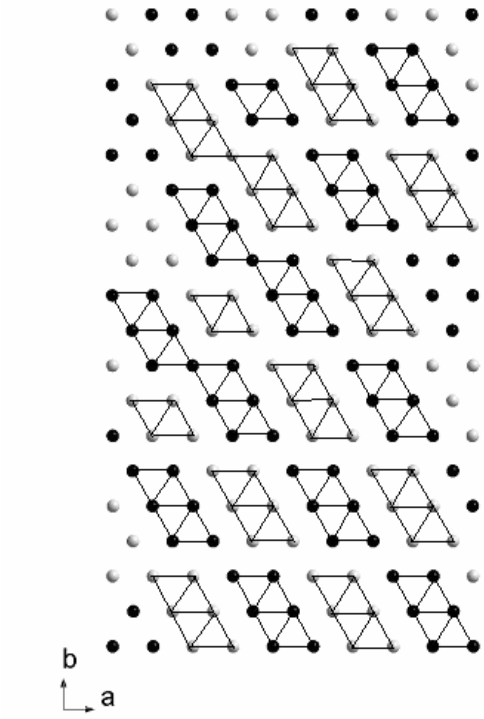

Fig. 6 Order of the Lu atoms (white $z = 0$; black $z = 1/2$) in $LuFe_6Ge_{2.5}Ga_{3.5}$ as deduced from refinements with JANA software (the $HfFe_6Ge_6$ blocks are emphasized).

2.6. The disordered YCo_6Ge_6-type structure and deviations from the idealized structures

The YCo_6Ge_6 type has been described as a filled derivative of the CoSn type, without any indication of long range ordering [36]. It is worth noting that some iron stannide and germanide superstructures have been observed later [29,30].

Some deviations from the idealized $HfFe_6Ge_6$ structure, or from the idealized orthorhombic structures, have been reported. According to Zaharko et al. [37], complete ordering of the M atoms is not observed in germanides. Mazet [38] reported a not fully occupied M site in the $HfFe_6Ge_6$-type compounds and related this to filling of anti-bonding states.

Interesting works have been devoted to the existence and shape of the satellites in the orthorhombic series [39,40]. In particular, an anisotropic broadening of the superstructure lines has been observed and the half-width of the peaks was found to be dependent on the annealing temperature.

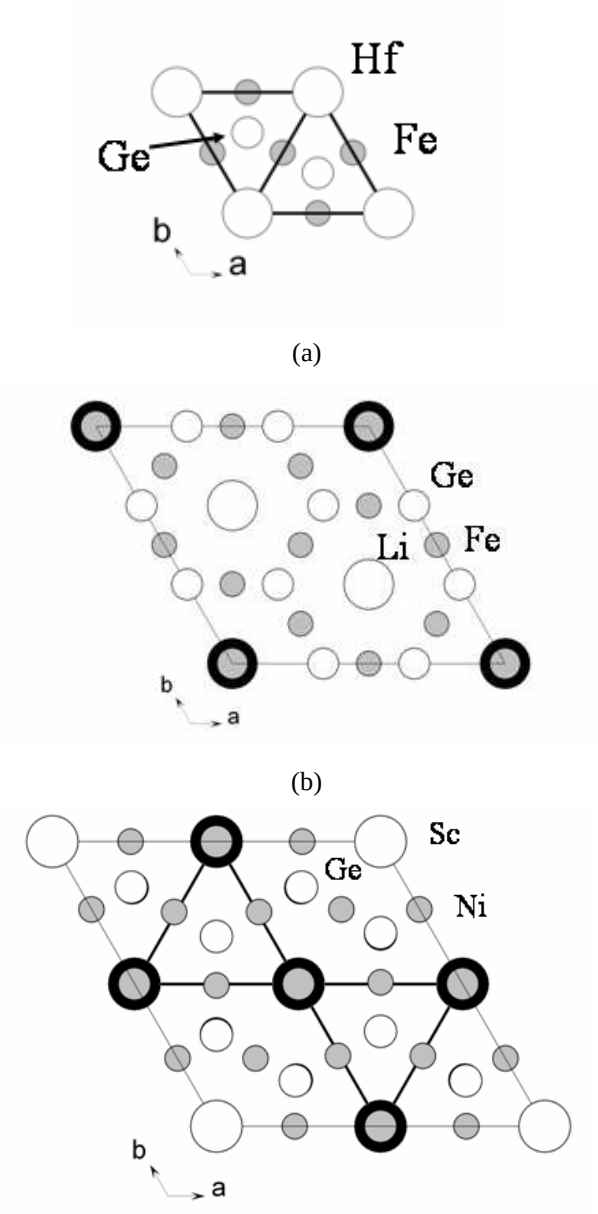

Fig. 7 Projections along [001] of the structures belonging to the hexagonal series: $HfFe_6Ge_6$ (a), $LiFe_6Ge_6$ (b), $ScNi_6Ge_6$ (c).

3. Crystal chemistry

3.1. Results of the structure refinements

3.1.1. Single crystal refinement of ternary MMn_6X_6 (X = Ge, Sn)

The atomic coordinates in hexagonal MMn_6X_6 (M = Sc, Tb, Er, Tm; X = Ge, Sn) compounds have been refined from single crystal diffraction for various M sizes [41,42]. The variation of the atomic coordinates as a function of the size of the M atom is summarized in Fig. 8. It was found that z_M is smaller in stannides than in germanides. This feature should account for a displacement of the Mn planes towards the M planes, thus suggesting bonding between the

two species. The z_X coordinate acts on the relative lengths of the M-X and X-X distances in the M-X-X-M chain running along the six-fold axes. For increasing X size, the variation of z_X indicathat the d_{X-X} distance increases to a larger extent than the d_{M-X} distance. The variation of z_X with the M size leads to an unusual variation of the X-X distance: it was found that d_{X-X} increases with decreasing cell volume (d_{Sn-Sn} = 2.98 Å and 2.93 Å for V = 233.6 Å^3 and 238.9 Å^3 in $ScMn_6Sn_6$ and $TbMn_6Sn_6$, respectively). This suggests that the X-X distances are too compressed when the M-X distance increases and that a smaller M atom enables a relaxation of the X-X distance. This feature should be a limiting factor concerning the stability of these phases for the largest M atoms.

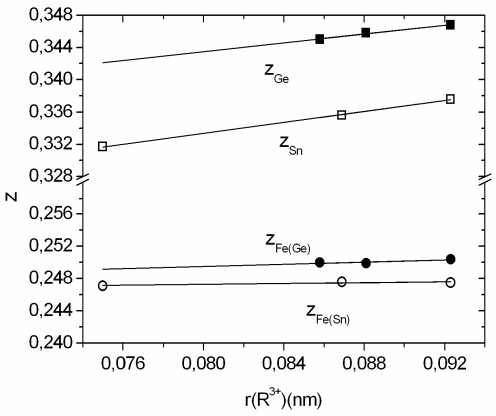

Fig. 8 Variation of the atomic coordinates in the $HfFe_6Ge_6$-type MMn_6Ge_6 and MMn_6Sn_6 single crystals as a function of the M ionic size.

3.1.2. Single crystal refinement of $DyFe_6Sn_6$ and powder refinement of $ErFe_6Sn_6$

An interesting single crystal refinement of the $DyFe_6Sn_6$ stannide has been undertaken by Oleksyn and Bohm [43]. This unique study, devoted to the orthorhombic compounds, provides information on the atomic coordinates in this series. Particularly, displacements of the Dy atoms are observed, yielding an increase of the thickness of the $HfFe_6Ge_6$ slabs with respect to the $ScFe_6Ga_6$ ones (Fig. 9). This leads to an increase of the Dy-Sn distances within the $HfFe_6Ge_6$ slab, thus suggesting that the stabilization of the orthorhombic phases might be an alternative to too short contacts between the M atom in 1(*a*) and the X atom in 2(*c*) in the hexagonal $HfFe_6Ge_6$-type compounds. The observation of orthorhombic compounds only for the largest M elements in manganese stannides should be related to a dilated Mn-Sn sublattice. A refinement of a powder sample of $ErFe_6Sn_6$ using the JANA software [33] led to the same conclusions.

3.1.3. Pseudo-ternary compounds

The distribution of the X and X' atoms has been checked for various pseudo-ternary compounds, using different experimental procedures. Neutron diffraction studies have been used for the (Ge,Ga) and (Sn,In) couples [44,45]. The contrast of the Fermi lengths is rather good for the (Sn,In) couple (L_{Sn}/L_{In} = 1.53), but less suitable for the (Ge,Ga) one (L_{Ge}/L_{Ga} = 1.12). The $MMn_6Sn_{6-x}Ga_x$ compounds have been studied by single crystal X-ray diffraction and the $MFe_6Sn_{6-x}Ge_x$ and $MFe_6Sn_{6-x}Ga_x$ compounds by powder X-ray diffraction [42,46,47]. Whatever X and X', it is observed that, when X' is larger than X, X' is mainly located in the 2(*d*) site and there is mainly an increase of the *c* parameter, whereas when X' is smaller than X, X' is mainly located in the 2(*c*) site, close to the 1(*a*) site of M, and both cell parameters decrease. In all cases, a decrease of the z_T coordinate is observed.

This leads to the following conclusions concerning the evolution of the interatomic distances. The $HfFe_6Ge_6$ type uses all its free variables (cell parameters and atomic coordinates) to adjust the M-X(X') and T-X(X') distances to the size of the X and X' atoms. Moreover, whatever the size of X', the M-T distance remains constant or decreases. This suggests that the site preference is driven by an optimization of this contact. This conclusion should be related to electronic structure calculations, which indicate hybridization between the 3dT and ndM states [48].

3.2. Structural evolution in pseudo-ternary compounds

3.2.1. $MT_6Sn_{6-x}Ge_x$ (M = RE element; T = Fe, Mn)

From the conclusions of section 3.1.3, it was expected that in the isoelectronic pseudo-ternary compounds $MT_6Sn_{6-x}Ge_x$, the small germanium atoms will occupy the 2(*c*) site to minimize the T-M distances. On the other hand, in section 3.1.2, it has been concluded that the occurrence of orthorhombic ternary stannides might be driven by a relaxation of the M-X(2*c*) contacts. These observations suggest that a transition from orthorhombic structures towards the hexagonal $HfFe_6Ge_6$ type might take place in Ge-doped stannides. This assumption has been checked and confirmed for the orthorhombic stannides $REFe_6Sn_6$ (RE = Gd-Er) and $REMn_6Sn_6$ (RE = Nd, Sm) [46,49]. The minimum concentration giving rise to a transition was checked for the $GdFe_6Sn_{6-x}Ge_x$ and the value x = 0.15 was found. This should enable comparative studies of the effect of crystallographic order on the magnetic properties.

3.2.2. $MFe_6Ge_{6-x}Ga_x$ (M = Sc, Tb, Lu) and $ErFe_6Sn_{6-x}In_x$

The MFe_6Ga_6 compounds (M = lanthanide) crystallize in the $ThMn_{12}$ structure, or in its ternary ordered derivative, the $ScFe_6Ga_6$ type. On the other hand, the MFe_6Ge_6 compounds crystallize either in the hexagonal $HfFe_6Ge_6$ type, or in orthorhombic types characterized by a large concentration of $HfFe_6Ge_6$ slabs. It seemed of interest to examine the

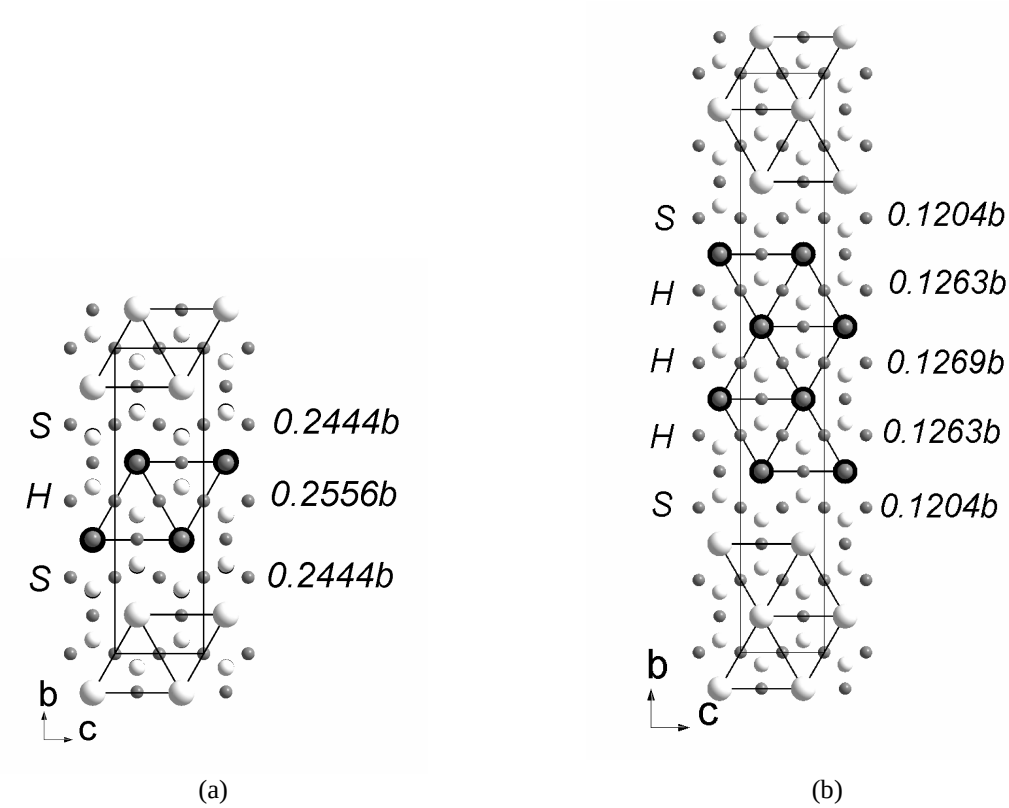

(a) (b)

Fig. 9 Projections of the refined $DyFe_6Sn_6$ (a) and $ErFe_6Sn_6$ (b) structures showing the thickness of the $HfFe_6Ge_6$ (H) and $ScFe_6Ga_6$ (S) slabs.

structural evolution among the pseudo-ternary $MFe_6Ge_{6-x}Ga_x$ compounds.

Investigations of various series (M = Sc, Tb, Lu) [31,32] clearly indicate a continuous structural evolution, displayed in Fig. 10. This study has evidenced a new monoclinic series, characterized by structures displaying a concentration of $ScFe_6Ga_6$ slabs greater than 1/2 and up to 5/6.

Recent investigations in the system $ErFe_6Sn_{6-x}In_x$ ($x < 1.5$) have shown the same tendency with a transition from the $ErFe_6Sn_6$ type (S/[H+S] = 1/4) towards the $HoFe_6Sn_6$ type (S/[H+S] = 1/3).

Although the role of the decreasing valence electron concentration (VEC) might be invoked, such an explanation disagrees with the occurrence of $HfFe_6Ge_6$-type MCr_6Ge_6 compounds [50], characterized by even smaller VEC. An alternative way to explain this phenomenon may be that the Ga or In atoms prefer the mono- and di-capped coordination of the $ScFe_6Ga_6$ slab. In this case, the new $ErFe_6Sn_{6-x}In_x$ compounds might be appropriate to check the site occupation, either by using the large contrast in Fermi lengths of tin and indium, or by using ^{119}Sn as local probe.

3.2.3. $MFe_6Sn_{6-x}Ga_x$ (M = Tb, Ho, Er)

Investigations in these series are interesting because gallium differs both by its smaller size and its different electronic structure.

The erbium series is characterized by a large concentration range ($0.25 < x_{Ga} < 2.5$) where the hexagonal $HfFe_6Ge_6$ structure is stabilized; powder refinements indicate that the gallium atoms are mainly located in the 2(*c*) site [47]. An increase of the atomic size of the M element leads to a different behavior. For the holmium series, the stability range is narrower ($1.0 < x_{Ga} < 1.5$) and there is no more stabilization of the hexagonal structure for the terbium series. This evolution suggests that in

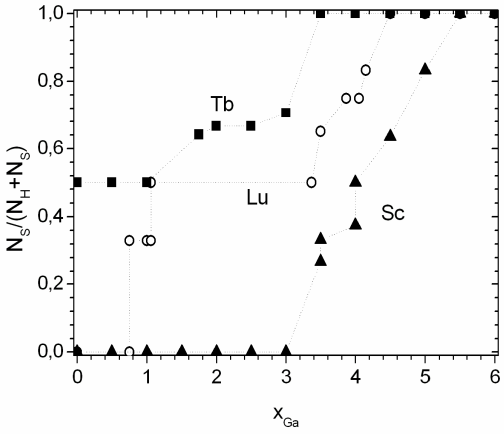

Fig. 10 Evolution of the concentration of $ScFe_6Ga_6$-slabs as a function of the gallium content in the compounds $MFe_6Ge_{6-x}Ga_x$ (M = Sc, Tb, Lu).

$MFe_6Sn_{6-x}Ga_x$ compounds there is effectively a competition between the size effect and the electronic effect and that this competition is tuned by the M size.

Preliminary powder refinements of the $TbFe_6Sn_6$-type $TbFe_6Sn_{6-x}Ga_x$ compounds ($0.5 < x < 1.5$) suggest that the gallium atoms are mainly located in the two Sn sites belonging to the $ScFe_6Ga_6$ slab and in the pseudo- 2(*c*) site of the $HfFe_6Ge_6$ slab.

4. Conclusions

The MT_6X_6 compounds display a rich crystal chemistry characterized by three structural series: the hexagonal, orthorhombic and monoclinic series. They account for different relative locations of the M atoms in the hexagonal channels of the CoSn host structure.

The various structure refinements undertaken on ternary and pseudo-ternary compounds emphasize the three preponderant hetero-atomic contacts T-X, M-X and M-T. In particular, it has been observed that the X' atoms are not randomly distributed on the three X sites of the $HfFe_6Ge_6$ structure, a feature which seems to be related to the M-T bonding and to the relative size of the X and X' atoms.

Besides this size effect, structural evolutions in systems $MFe_6Ge_{6-x}Ga_x$ and $MFe_6Sn_{6-x}In_x$ have also been observed, which can be related to the electronic structure of the X' element. This phenomenon is still not well understood and will need further investigations.

Finally, it seems that optimized substitutions should enable the stabilization of "taylor-cut" samples, in order to check the variation of the physical properties as a function of the crystallographic order.

References

[1] R.V. Skolozdra, O.E. Koretskaya, *Ukr. Fiz. Zh.* 29 (1984) 877.

[2] F. Weitzer, A. Leithejasper, K. Hiebl, P. Rogl, Q.N. Qi, J.M.D. Coey, *J. Appl. Phys.* 73(13) (1993) 8447.

[3] P. Tils, M. Loewenhaupt, K.H.J. Buschow, R.S. Eccleston, *J. Alloys Compd.* 279(2) (1998) 123.

[4] G. Venturini, D. Fruchart, B. Malaman, *J. Alloys Compd.* 236 (1996) 102.

[5] F.M. Mulder, R.C. Thiel, J.H.V.J. Brabers, F.R. de Boer, K.H.J. Buschow, *J. Alloys Compd.* 190 (1993) L29.

[6] Y. Amako, T. Yamamoto, H. Nagai, *Hyperfine Interact.* 94 (1994) 1897.

[7] A.P. Gonçalves, J.C. Waerenborgh, G. Bonfait, A. Amaro, M.M. Godinho, M. Almeida, J.C. Spirlet, *J. Alloys Compd.* 204 (1994) 59.

[8] Y. Li, R.G. Bunbury, P.W. Mitchell, M.A.H. Mc Causland, R.S. Chaughule, L.C. Gupta, R. Vijayaraghavan, C. Godart, *J. Magn. Magn. Mater.* 140-144 (1995) 1031.

[9] J.F. Hu, K.Y. Wang, B.P. Hu, Y.Z. Wang, Z.X. Wang, F.M. Yang, N. Tang, R.W. Zhao, W.D. Qin, *J. Phys.: Condens. Matter* 7(5) (1995) 889.

[10] D.H. Ryan, J.M. Cadogan, *J. Appl. Phys.* 79(8) (1996) 6004.

[11] P. Rösch, M.T. Kelemen, B. Pilawa, E. Dormann, K.H.J. Buschow, *J. Magn. Magn. Mater.* 164 (1996) 175.

[12] R. Duraj, A. Szytula, G. Venturini, *Phys. Status Solidi B* 236(2) (2003) 466.

[13] B. Malaman, G. Venturini, R. Welter, J.P. Sanchez, P. Vuillet, E. Ressouche, *J. Magn. Magn. Mater.* 202 (1999) 519.

[14] D.M. Clatterbuck, R.J. Lange, K.A. Gschneidner Jr, *J. Magn. Magn. Mater.* 195(3) (1999) 639.

[15] J. Han, G.K. Marasinghe, W.J. James, M. Chen, W.B. Yelon, I. Dubenko, N. Ali, *J. Appl. Phys.* 87(9) (2000) 5281.

[16] N.K. Zajkov, N.V. Mushnikov, M.I. Bartashevich, T. Goto, *J. Alloys Compd.* 309 (2000) 26.

[17] N.K. Zaikov, A.N. Pirogov, N.V. Mushnikov, A.E. Teplykh, E.Z. Valiev, Yu.A. Dorofeev, *JETP Lett.* (translation of *Pis'ma Zh. Eks. Teor. Fiz.*) 72(8) (2000) 436.

[18] A. Mar, C. Lefèvre, G. Venturini, *J. Magn. Magn. Mater.* 269 (2004) 380.

[19] S.Y. Zhang, P. Zhao, Z.H. Cheng, R.W. Li, J.R. Sun, H.W. Zhang, B.G. Shen, *Phys. Rev. B* 64 (2001) 212404-1.

[20] Y. Shigeno, K. Kaneko, T. Hori, Y. Iguchi, Y. Yamaguchi, T. Sakon, M. Motokawa, *J. Magn. Magn. Mater.* 226-230 (2001) 1153.

[21] F. Canepa, M. Napoletano, R. Masini, C. Lefèvre, G. Venturini, *J. Phys.: Condens. Matter* 17 (2005) 1961.

[22] L. Zhang, J.C.P. Klasse, E. Brück, K.H.J. Buschow, F.R. de Boer, S. Yoshii, K. Kindo, C. Lefèvre, G. Venturini, *Phys. Rev. B* 70 (2004) 2244251-9.

[23] O. Nial, *Z. Anorg. Allg. Chem.* 238 (1938) 287.

[24] R.R. Olenych, L.G. Aksel'rud, Ya.P. Yarmolyuk, *Dopov. Akad. Nauk Ukr. RSR, Ser. A* 43(2) (1981) 87.

[25] W. Buchholz, H.U. Schuster, *Z. Naturforsch. B* 33 (1978) 877.

[26] B. Malaman, B. Roques, A. Courtois, *J. Protas, Acta Crystallogr. B* 32 (1976) 1352.

[27] N.N. Beljavina, V.Ya. Markiv, *Dopov. Akad. Nauk Ukr. RSR, Ser. B* (12) (1982) 31.

[28] J.V. Florio, R.E. Rundle, A.I. Snow, *Acta Crystallogr.* 5 (1952) 449.

[29] B. Chafik El Idrissi, G. Venturini, B. Malaman, *Mater. Res. Bull.* 26(12) (1991) 1331.

[30] G. Venturini, R. Welter, B. Malaman, *J. Alloys Compd.* 185 (1992) 99.
[31] G. Venturini, *J. Alloys Compd*. 322 (2001) 190.
[32] G. Venturini, *J. Alloys Compd*. 329 (2001) 8.
[33] V. Petricek, M. Dusek, *Z. Kristallogr.* 219(11) (2004) 692.
[34] E. Welk, H.U. Schuster, *Z. Anorg. Allg. Chem.* 424(3) (1976) 193.
[35] W. Buchholz, H.U. Schuster, *Z. Anorg. Allg. Chem.* 482 (1981) 40.
[36] O.Ya. Mruz, P.K. Starodub, O.I. Bodak, *Dopov. Akad. Nauk Ukr. RSR, Ser. B* (12) (1984) 45.
[37] O. Zaharko, P. Schobinger-Papamantellos, J. Rodriguez-Carvajal, K.H.J. Buschow, *J. Alloys Compd.* 288(1-2) (1999) 50.
[38] T. Mazet, *Ph.D. Thesis*, Nancy, 2000.
[39] P. Schobinger-Papamantellos, O. Oleksyn, J. Rodriguez-Carvajal, G. André, E. Bruck, K.H.J. Buschow, *J. Magn. Magn. Mater.* 182(1-2) (1998) 96.
[40] O. Zaharko, P. Schobinger-Papamantellos, C. Ritter, J. Rodriguez-Carvajal, K.H.J. Buschow, *J. Magn. Magn. Mater.* 187 (1998) 293.
[41] B. Chafik El Idrissi, G. Venturini, B. Malaman, *Mater. Res. Bull.* 26 (1991) 431.
[42] C. Lefèvre, G. Venturini, B. Malaman, *J. Alloys Compd.* 354(1-2) (2003) 47.
[43] O. Oleksyn, H. Bohm, *Z. Kristallogr.* 213(5) (1998) 270.
[44] C. Lefèvre, G. Venturini, B. Malaman, *J. Alloys Compd.* 343 (2002) 38.
[45] C. Lefèvre, G. Venturini, B. Malaman, *J. Alloys Compd.* 361 (2003) 40.
[46] G. Venturini, *J. Alloys Compd*. 400 (2005) 37.
[47] H. Ihou-Mouko, G. Venturini, *J. Alloys Compd.* 396 (2005) 59.
[48] T. Mazet, J. Tobola, B. Malaman, *Eur. Phys. J. B* 33(2) (2003) 183.
[49] G. Venturini, *J. Alloys Compd*. 398 (2005) 42.
[50] J.H.V.J. Brabers, K.H.J. Buschow, F.R. de Boer, *J. Alloys Compd.* 205 (1994) 77.

Proceeding of the IX International Conference on Crystal Chemistry of Intermetallic Compounds, Lviv, September 20-24, 2005.